NACA

RESEARCH MEMORANDUM

FORCES AND MOMENTS ON POINTED AND BLUNT-NOSED BODIES

OF REVOLUTION AT MACH NUMBERS FROM 2.75 TO 5.00

By David H. Dennis and Bernard E. Cunningham

Ames Aeronautical Laboratory Moffett Field, Calif.

NATIONAL ADVISORY COMMITTEE FOR AERONAUTICS

WASHINGTON

August 8, 1952 Declassified July 2, 1958

NATIONAL ADVISORY COMMITTEE FOR AERONAUTICS

RESEARCH MEMORANDUM

FORCES AND MOMENTS ON POINTED AND BLUNT-NOSED BODIES

OF REVOLUTION AT MACH NUMBERS FROM 2.75 TO 5.00

By David H. Dennis and Bernard E. Cunningham

SUMMARY

Results of force and moment tests at Mach numbers from 2.75 to 5.00 on pointed and blunt-nosed bodies of revolution are presented and compared with predictions of the second-order cone theory of Stone and the impact theory of Newton. Cones and tangent ogives of fineness ratios from 3 to 7, and blunt-nosed shapes having fineness ratios of 3 and 5, were tested at angles of attack from 0° to 25°. Reynolds numbers based on body length varied from 0.5 million to 6.4 million, depending on body fineness ratio and test Mach number.

Comparisons of force characteristics of the various body shapes show that the blunt-nosed shapes are generally more efficient lifting bodies, from the standpoint of lift-drag ratios, than the cones or ogives of the same fineness ratio. It is also found throughout the Mach number range that within the range of fineness ratios tested, increasing body fineness ratio results in higher lift-drag ratios.

Predictions of the inclined-cone theory of Stone are found to agree well with experimentally determined characteristics of cones up to angles of attack equal to their semiapex angles. At higher angles of attack the measured lifts and increments of drag are higher than predicted by the theory. Throughout the angle-of-attack range the impact theory predicts lower lift and higher increments of drag than measured, but, as might be expected, the agreement between theory and experiment improves with increasing Mach number.

INTRODUCTION

The attainment of higher supersonic speeds by missiles has been accompanied by a trend toward configurations consisting principally of a body, with small planar surfaces attached primarily for the purpose of

achieving stable and controlled flight. It is evident, of course, that the resultant aerodynamic forces acting on such a configuration are contributed in large part by the body. Hence, it may be expected that accurate knowledge of the forces and attendant moments acting on inclined bodies will be essential to the proper design of missiles operating at high supersonic Mach numbers.

At present, however, information on inclined body characteristics at high Mach numbers is restricted to that obtainable from approximate theories and to that provided by a limited number of experiments. Of the available theories for predicting the forces and moments on inclined bodies, perhaps the most suitable at the Mach numbers under consideration are those of Stone and Ferri for cones (references 1 and 2, respectively) and that of Newton (i.e., the impact theory, reference 3) for bodies of arbitrary shape. In general, however, the former theories are not applicable to comes inclined at large angles with respect to the free stream, while the Newtonian theory cannot be expected to apply accurately to typical body shapes unless the free-stream Mach number is very large compared to 1 (i.e., the flight speed is hypersonic). Thus it is evident that theory, as now developed, does not adequately provide the desired aerodynamic information. In the case of experiment, some data for inclined bodies are available for Mach numbers of about 4 (see, e.g., references 4 and 5) but only limited tests at higher Mach numbers have been reported (see reference 6). In all the tests at high supersonic speeds reported to date, body shapes have been restricted to cone or ogive cylinders and only a few detailed comparisons with theories have been made.

It is evident, then, that more information of both an experimental and theoretical nature is needed on the aerodynamic characteristics of inclined bodies at high supersonic speeds. As a step in the direction toward providing this information, an experimental program to determine the aerodynamic characteristics of bodies of revolution at angles of attack from 0° to 25° and Mach numbers from 2.7 to 5 was undertaken. The first phase of this program, reported herein, concerns the determination of the force and pitching-moment characteristics of pointed nose sections of fineness ratios from 3 to 7 and blunt-tipped nose sections of fineness ratios 3 and 5. A comparison of these characteristics with those predicted by the theories previously discussed is also included.

SYMBOLS

$$c_{D}$$
 drag coefficient $\left(\frac{D}{q\pi r_{b}^{2}}\right)$

2

 $\triangle \mathtt{C}_{D}$ $\;$ increment of drag coefficient due to angle of attack

- C_{L} lift coefficient $\left(\frac{L}{q_{\pi}r_{b}^{2}}\right)$
- C_{m} pitching-moment coefficient about body nose $\left(\frac{\text{pitching moment}}{q\pi r_{b}^{2}l}\right)$
- c.p. center of pressure location, percent body length from nose
- D body drag
- f body fineness ratio $\left(\frac{l}{2r_b}\right)$
- L body lift
- M free-stream Mach number
- l body length
- q free-stream dynamic pressure
- r body radius
- rb radius of body at base
- Re Reynolds number based on body length
- x axial distance measured from body nose
- n exponent in equation defining body shapes
- α angle of attack

EXPERIMENT

Test Apparatus and Methods

The tests were conducted in the Ames 10- by 14-inch supersonic wind tunnel which is a continuous flow, nonreturn-type tunnel, operating with a nominal supply pressure of 6 atmospheres. By changing the relative positions of the symmetrical top and bottom walls of the wind tunnel, the Mach number in the test section may be varied from approximately 2.7 to 5.0. A detailed description of the wind tunnel and its associated equipment may be found in reference 7.

Aerodynamic forces and moments were measured by a three-component strain-gage balance. Forces parallel and perpendicular to the balance

axis and moments about points slightly downstream of the body bases were determined directly. These forces were resolved to give pitching moments about the body noses and lift and drag forces normal to and parallel with the free-stream direction, respectively. Angles of attack greater than the 45° obtainable by rotating the model-balance assembly were reached with the aid of bent-sting model supports. Tare forces on the sting supports were eliminated by enclosing the stings in shrouds that extended to within 0.040 inch of the model base.

Forces acting on the bases of the models were determined from base-pressure readings made with the aid of a McLeod gage. These forces were subtracted from measured total forces; thus, the data presented include only the aerodynamic forces and moments acting on the portions of the test bodies ahead of the bases.

Static and dynamic pressures in the test section were determined from wind-tunnel calibration data and stagnation pressures measured with a Bourdon type pressure gage.

Models

Tangent ogive shapes and shapes defined by the equation

$$r = r_b \left(\frac{x}{l}\right)^n$$

for values of n equal to 1, 3/4, and 1/2 were tested. Thus, there are included two pointed-nosed shapes, conical (n=1) and ogival, and two blunt-nosed shapes, slightly blunt (n=3/4) and parabolic (n=1/2). To compare the shapes of these bodies, a sketch of the profiles of fineness ratio 3 is shown in figure 1(a). Figure 1(b) is a photograph of the 11 test bodies; the fineness ratios 3, 4, 5, and 7 cones, fineness ratios 3 and 5 3/4-power and 1/2-power blunt bodies, and the fineness ratios 3, 5, and 7 tangent ogives. All models were of polished steel and had base diameters of 1 inch.

The cones and ogives were employed since they are representative of nose sections commonly used on missiles. Also, it may be noted that the cone is an approximation to the minimum drag body of revolution for given base diameter and surface area at high supersonic speeds (see reference 7). The 3/4-power bodies (n = 3/4) were included particularly to determine experimentally if the advantage of very low drag (for a given fineness ratio) at zero lift exhibited by this shape (see reference 7) results in a more efficient lifting body than those commonly used. The 1/2-power bodies were chosen since they are sufficiently blunt at the nose to facilitate the installation of a seeker, while having relatively low

zero-lift drag (less, for example, than the ogive of the same fineness ratio; see reference 7). In addition, it is clear that tests on these bodies provide means of determining the accuracy of existing inclined-cone theory and the applicability of the impact theory to bodies of a fairly wide range of shapes in the test Mach number range.

Accuracy of Test Results

Variations in Mach number in the region of the test section where models were located did not exceed ±0.06 at any test condition and, in general, deviations from nominal Mach numbers were not greater than ±0.03. Corresponding variations in stream static pressure were sufficiently small so that buoyancy corrections were necessary only for the measured drags at Mach number 2.75.

Deviations in free-stream Reynolds number for a given Mach number from the values shown in figure 2 did not exceed ±30,000.

The estimated errors in the angle-of-attack values due to uncertainties in corrections for stream angle and for deflections of the model-support system were $\pm 0.2^{\circ}$.

Precision of the computed force coefficients was affected both by inaccurate measurements of the aerodynamic forces by the balance system, and by uncertainties in the determination of free-stream dynamic pressures and base pressures. These uncertainties may result in maximum errors in lift and drag coefficients at the high angles of attack of ±0.008 at Mach numbers from 2.7 to 4.5, and ±0.035 at Mach number 5.0. At angles of attack less than about 10° the corresponding maximum errors are ±0.004 and ±0.015, respectively. Possible errors in moment coefficients, due mainly to errors in measured lift, were of the same magnitude as errors in lift coefficients.

It should be noted that the above discussion concerns maximum errors and that, in general, the results presented are in error by less than half of the foregoing estimates.

A possible additional uncertainty in the results presented for M = 5.00 is due to the presence of a small amount of condensed air in the stream. A detailed discussion of condensation in the 10- by 14-inch supersonic wind tunnel and its effects on the forces acting on models may be found in reference 8. In this paper it was shown that for a body of revolution at zero angle of attack and for wedge airfoils, the change in surface pressure due to condensed air in the flow is of the same magnitude as that caused by the effective change in body shape due to boundary-layer growth. In view of this result, it seems logical to expect that the

corresponding pressure change on inclined bodies would be small (not exceeding about 10 percent at high angle of attack). As will be observed later, the forces on models were influenced to a relatively small extent by the presence of condensed air.

6

Presentation of Test Results

Because only experimental results typical of those obtained during this investigation are presented in the following discussion, a large portion of the data is not shown in graphical form. All the experimental results of the tests are presented in tables I to XI. Lift, drag, and pitching-moment coefficients, centers of pressure, and lift-drag ratios at the several test Mach numbers are tabulated for each of the ll test bodies at various angles of attack.

DISCUSSION OF RESULTS

Experimental Results

Characteristics of cones. To illustrate the effects of fineness ratio on the aerodynamic characteristics of the test bodies, the variations of lift coefficient with angle of attack, with drag coefficient, and with center of pressure for cones of fineness ratios 3, 4, 5, and 7 are shown in figure 3. It may be seen that throughout the test Mach number range the variation of lift coefficient with angle of attack does not change appreciably with cone fineness ratio up to angles of attack of 4°to 5°. At 5° and above the data show that increasing the fineness ratio results in appreciably higher lift coefficients. It is also evident that, although the lift coefficients increase slightly with increasing Mach number at very small angles of attack, the lift coefficients generally decrease with increasing Mach number at angles of attack greater than approximately 10°.

The curves in figure 3 which present the variations of lift coefficient with drag coefficient show that, within the range of fineness ratios tested, increasing fineness ratio results in lower zero-lift drag and lower increments of drag for given increments of lift throughout the Mach number and angle-of-attack ranges. It may also be seen that for a given angle of attack, the drag coefficients of the long cones do not exceed those of the shorter cones until the angles of attack exceed about 15°.

Centers of pressure are approximately the same for all cones tested and, within the ranges of lift coefficient where accurate

center-of-pressure data were obtained, there is little or no shift of centers of pressure with increasing lift or with changes in Mach number.

To show the variation of lifting efficiency with body fineness ratio, the lift-drag ratios of the several cones at Mach number 4.01 are shown as a function of lift coefficient in figure 4. It is clear that, within the range of fineness ratios tested, the lift-drag ratios increase with increasing cone fineness ratio. The maximum lift-drag ratios occur at approximately the same value of lift coefficient ($C_L \approx 0.32$) for all of the cones. Furthermore, the angles of attack for maximum L/D vary only from 8° for the fineness ratio 7 cone to 10° for the fineness ratio 3 cone.

The effects of Mach number variation on lift-drag ratio are indicated in figure 5 where the lift-drag ratios of the fineness ratio 5 cone are plotted with respect to lift coefficient for the several test Mach numbers. It is evident that at high lift coefficients, lift-drag ratio decreases with increasing Mach number. Maximum lift-drag ratio occurs, under the conditions of the present tests, at Mach number 4.01. However, the large changes of Reynolds number with Mach number and the resultant variation of skin-friction drag may have comparatively large effects on the variation of maximum lift-drag ratio with Mach number. Thus the variation of L/Dmax with Mach number at constant Reynolds number would probably be somewhat different from that shown in figure 5.

Effects of profile shape. The effects on aerodynamic characteristics of changes in profile shape of bodies of given fineness ratio are shown in figures 6, 7, 8, and 9. Variations of lift coefficient with angle of attack, drag coefficient, and center of pressure, and variations of lift-drag ratio with lift coefficient are presented for the fineness ratio 3 bodies at Mach numbers 2.75, 4.01, and 5.00 in figures 6, 7, and 8, respectively, and for the fineness ratio 5 bodies at Mach number 4.01 in figure 9.

At a given angle of inclination, lift coefficients vary with body shape approximately as body plan-form area. For example, at a given Mach number the ogives and 1/2-power bodies which have very nearly the same plan-form area have approximately the same lift throughout the angle-of-attack range, while the 3/4-power bodies and cones have lower lift by

¹Center-of-pressure data at low values of lift coefficient and at M = 5.00 are subject to considerable error due to uncertainties in measurements of the very small lift and moment.

It should be noted that the variation with Mach number of the lift coefficient for $L/D_{\rm max}$ is similar to that predicted by the inclined cone theory of Stone. The variation of lift-drag ratio with Mach number at high lift coefficients is also in agreement with that given by Stone.

approximately the same percentages that their plan-form areas differ from those of the ogives and 1/2-power bodies.

It may be seen in the polar curves that the 3/4-power bodies, due to their low drag, are the most efficient lifting bodies at low angles of attack. However, the increase in drag with a given increment of lift is greater for these bodies and for the cones than for the 1/2-power and ogive bodies of the same fineness ratio at the higher angles of attack. This is reflected in the lift-drag-ratio curves (figs. 6(b), 7(b), 8(b), and 9(b)) where it is seen that, at large values of lift coefficient, the 1/2-power and ogive shapes are more efficient lifting shapes than the 3/4-power bodies and cones. It should be noted that the relatively low values of lift-drag ratio for the fineness ratio 3 bodies at Mach number 5.00 (fig. 8(b)) are due to the low test Reynolds number and the attendant high friction drag at this Mach number.

The centers of pressure are relatively unaffected by changes of lift coefficient, at least within the range of angle of attack where slight uncertainties in lift and pitching moment did not result in large errors in center-of-pressure determinations.

In general, the results in figures 6 to 9 show that the force characteristics of the cones and the 3/4-power bodies are somewhat similar and those of the ogives and 1/2-power bodies are similar. Furthermore, the blunt-nosed shapes of these two pairs are better than the corresponding sharp-nosed shapes from the standpoint of lower drag for a given lift coefficient throughout the test angle-of-attack range. The test results also show that up to lift coefficients of approximately 0.5 the 3/4-power bodies, which for a given fineness ratio have minimum drag at zero lift (see reference 7), retain their low-drag advantage and have the highest lift-drag ratios of the bodies tested.

Comparisons of Theory With Experiment

Characteristics of cones. - Experimental results showing the variation of lift coefficient with angle of attack, increment of drag coefficient, and center of pressure for fineness ratios 3 and 5 cones are compared in figure 10 with Stone's second-order theory and with impact

The tabulated values of references 9, 10, and 11 were used in conjunction with equations (21) and (22) (for drag and lift-force coefficients, respectively) of reference 12. This procedure was necessary to transfer the coordinate system from wind axes used in references 10 and 11 to body axes.

theory. For these comparisons, values of increments of drag coefficient have been shown rather than total foredrag coefficients because friction drag is not taken into account by these theories. The data in figure 10 show that the inclined-cone theory of Stone predicts with good accuracy the variation of lift with angle of attack up to angles equal to about the half-cone angles (9.46° for the fineness ratio 3 cone and 5.74° for the fineness ratio 5 cone). Increments of drag due to lift are predicted by the inclined-cone theory with good accuracy up to larger angles. In fact, agreement between theoretical and experimental drag polars is good up to experimental lift coefficients corresponding to angles of attack of 15° to 20°. It should be noted, however, that the agreement of polars (particularly in the case of the fineness ratio 5 cone) is due to low theoretical predictions both of lift and of increment of drag in the high angle-of-attack range.

The impact theory generally predicts lower lift coefficients but higher increments of drag coefficient due to lift than measured experimentally. The variation of increment of drag with angle of attack, however, is relatively accurately predicted. It is not to be expected, of course, that the impact theory should apply accurately at these relatively low Mach numbers. It is interesting to note, however, that with increasing Mach number the magnitudes of the measured force coefficients approach those predicted by the impact theory. The comparisons between impact theory and experimental results at M = 6.86 presented in reference 6 indicate that this trend continues to that Mach number.

Both the cone theory and the impact theory predict the center of pressure at a point two-thirds the cone length from the apex. The experimental results show the center of pressure to be very slightly aft (less than 3 percent of body length) of the predicted location throughout the angle-of-attack range.

Characteristics of blunt-nosed and ogive bodies.- Comparisons of typical results of the impact theory and experiment for the characteristics of the 3/4-power, 1/2-power, and ogive bodies are shown in figure 11. The trend noted in the consideration of the cone results is again evident. That is, with increasing Mach number, body force characteristics approach those predicted by the impact theory. In this connection, it is observed also that the impact theory is in somewhat better

Equations developed by Grimminger, Williams, and Young (reference 13) were used for all impact-theory calculations in the present paper. Pressure coefficients on the lee or "shaded" portions of the bodies were assumed to be zero and centrifugal-force effects were neglected.

It is tacitly assumed that the contribution of friction drag to total drag does not vary appreciably within a moderately large angle-of-attack range. It is also noted that comparison of drag increments eliminates errors in the prediction of zero lift pressure drag by the impact theory (see reference 7).

agreement with experiment at Mach number 5.00 for these bodies than for the cones. This result is most probably due to the fact that the flow in the region of the noses of these bodies, by virtue of their relative bluntness, has more nearly the characteristics of a truly hypersonic flow than in the case of the cones. Again the centers of pressure are very slightly aft of the locations predicted theoretically.

The relatively good agreement between the predictions of the impact theory and the experimental results at the higher test Mach numbers must be considered at least partly fortuitous, since these Mach numbers are considerably lower than those for which the theory would be expected to apply with reasonable accuracy. This agreement probably results primarily because the differences between the flow conditions assumed in the development of the theory and those that actually exist, in general, have compensating effects on the aerodynamic forces on bodies. For example, the pressure coefficients on the lee portions of the bodies are assumed to be zero, while under the test conditions these pressure coefficients are probably slightly negative (see, e.g., reference 4). On the other hand, the neglect, by the theory, of centrifugal relieving forces which exist on the windward sides of the bodies tends to offset this discrepancy. Similarly, the neglect of friction forces may be partly compensated for by an incomplete transformation of the normal component of momentum to pressure forces.

An additional factor having perhaps a small favorable effect on the agreement between impact theory and experiment at Mach number 5.00 is the presence of condensed air in the flow. The change in forces due to condensed air is caused by re-evaporation of the condensed phase as it passes through the bow wave, thus bringing about a small decrease in pressure on the windward sides of the models. In addition, the pressures on the lee sides may not decrease to the normal extent if recondensation takes place.

CONCLUSIONS

Analysis of the results of tests at Mach numbers from 2.75 to 5.00 on inclined bodies of revolution in the Ames 10- by 14-inch supersonic wind tunnel has led to the following conclusions:

- 1. Within the ranges of fineness ratio and Mach number of the tests, the lift-drag ratios of bodies of similar shape increase with increasing fineness ratio.
- 2. At high lift coefficients the lift-drag ratio of a given body decreases with increasing Mach number.

- 3. At high angles of inclination the lift coefficient on bodies of equal fineness ratio varies approximately as the plan-form areas of the bodies.
- 4. The blunt-nosed bodies tested are generally more efficient lifting bodies, from the standpoint of lift-drag ratio, than are the pointed-nosed cone and ogive shapes of the same fineness ratio.
- 5. The 3/4-power body which, for a given fineness ratio has minimum zero-lift drag at high supersonic speeds, has the greatest L/D_{max} of the bodies tested.
- 6. The second-order inclined-cone theory of Stone adequately predicts the variations with angle of attack of lift, increment of drag, and center of pressure up to angles approximately equal to the semiapex angles of the cones.
- 7. With increasing Mach number the aerodynamic characteristics of all models approach those predicted by the impact theory. The agreement at M = 5.00 between impact theory and experiment is somewhat better for the ogive and blunt-tipped shapes than for the cones.

Ames Aeronautical Laboratory
National Advisory Committee for Aeronautics
Moffett Field, Calif.

REFERENCES

- 1. Stone, A. H.: On Supersonic Flow Past a Slightly Yawing Cone. Jour. Math. and Phys., vol. 27, no. 1, Apr. 1948, pp. 67-81.
- 2. Ferri, Antonio: Supersonic Flow Around Circular Cones at Angles of Attack. NACA TN 2236, 1950.
- 3. Newton, Isaac: Principia Motte's Translation Revised. University of California Press, 1946, pp. 333, 657-661.
- 4. Lord, Douglas R., and Ulmann, Edward F.: Pressure Measurements on an Ogive-Cylinder Body at Mach Number 4.04. NACA RM L51L20, 1952.
- 5. DeMeritte, F. J., and Darling, J. A.: Aeroballistic Investigation of Body-Alone Models at Mach Numbers 4.38 and 2.92. Naval Ordnance Laboratory, Memo. 10132, May 1950.

- 6. Cooper, Ralph D., and Robinson, Raymond A.: An Investigation of the Aerodynamic Characteristics of a Series of Cone-Cylinder Configurations at a Mach Number of 6.86. NACA RM L51J09, 1951.
- 7. Eggers, A. J., Jr., Dennis, David H., and Resnikoff, Meyer M.:
 Bodies of Revolution for Minimum Drag at High Supersonic Airspeeds. NACA RM A51K27, 1952.
- 8. Hansen, C. Frederick, and Nothwang, George J.: Condensation of Air in Supersonic Wind Tunnels and Its Effects on Flow About Models. NACA TN 2690, 1952.
- 9. Mass. Inst. Tech., Dept. Elec. Engr., Center of Analysis. Tables of Supersonic Flow Around Cones. By the staff of the Computing Section, Center of Analysis, under the direction of Zdenek Kopal. Cambridge, 1947. (Tech. Rep. No.1)
- 10. Mass. Inst. Tech., Dept. Elec. Engr., Center of Analysis. Tables of Supersonic Flow Around Yawing Cones. By the staff of the Computing Section, Center of Analysis, under the direction of Zdenek Kopal. Cambridge, 1947. (Tech. Rep. No. 3)
- 11. Mass. Inst. Tech., Dept. Elec. Engr., Center of Analysis. Tables of Supersonic Flow Around Cones of Large Yaw. By the staff of the Computing Section, Center of Analysis, under the direction of Zdenek Kopal. Cambridge, 1949. (Tech. Rep. No. 5)
- 12. Young, G. B. W., and Siska, C. P.: Supersonic Flow Around Cones at Large Yaw. Rand Corporation P-198, Mar. 1, 1951.
- 13. Grimminger, G., Williams, E. P., and Young, G. B. W.: Lift on Inclined Bodies of Revolution in Hypersonic Flow. Jour. Aero. Sci., vol. 17, no. 11, Nov. 1950, pp. 675-690.

TABLE I.- EXPERIMENTAL RESULTS, CONE, FINENESS RATIO 3

М	α	$C_{ m L}$	c_{D}	Cm	L/D	c.p.	M	α	CL	c_{D}	Cm	L/D	c.p.
2.75	-1.0 0 1.0 3.0 5.0 5.3 7.8	002 .028 .086 .140	.102	-0.020 062 099 114	-0.030 016 .300 .845 1.26 1.40	67.6 67.8 66.7 68.5	4.01	12.3 14.1 15.4 16.2 20.1 23.2	0.392 .450 .503 .520 .644 .723	0.185 .221 .258 .277 .395 .483	-0.292 338 382 391 501 589	2.12 2.04 1.94 1.88 1.63 1.50	69.2 69.0 68.9 67.8 67.6
	10.3 12.9 15.1 15.4 15.4 20.2 25.3	.232 .318 .413 .513 .518 .506 .714 .877	.130 .157 .196 .239 .243 .245 .382	169 234 307 388 397 382 558 718	1.79 2.02 2.10 2.15 2.13 2.07 1.87 1.56	68.2 68.7 68.8 69.5 70.4 69.1 69.6 69.7	4.48	-1.0 0 1.0 2.2 2.8 5.0 7.8	027 002 .026 .038 .075 .134 .228	.088 .087 .096 .096 .109	028 060 094 165	306 019 .298 .394 .786 1.22 1.68	67.0 75.3 65.8 67.7
3. h9	-1.0 0 1.0 3.0 5.0 5.3 7.8 10.3 12.9	.002 .028 .086 .145 .151 .232	.084 .084 .084 .093 .104 .101 .123 .152		325 .021 .336 .927 1.40 1.50 1.89 2.06 2.08	68.2 68.0 68.2 67.0 67.3 68.0		8.3 10.3 11.8 13.2 15.3 17.1 18.1 20.1 22.1	.257 .326 .376 .423 .487 .550 .582 .643	.134 .162 .185 .210 .260 .312 .336 .394 .462	193 247 288 329 379 433 443 490 539	1.91 2.01 2.03 2.01 1.88 1.76 1.73 1.63	70.1 70.5 71.6 70.1 70.1 66.3 65.3
4.01	-1.0 0 1.0 3.0 3.0 4.0 5.0 6.5 7.0 8.3	023 .006 .028 .090 .089 .118 .151	.246 .089 .088 .088 .096 .098 .099 .110 .116	373 	2.02 261 .065 .320 1.02 .927 1.20 1.52 1.86 1.84 2.07	68.6 	5.00	85 .13 1.1 1.9 2.5 4.9 6.8 9.7 13.3 17.3	007 .005 .046 .068 .104 .169 .221 .301 .417 .470	.106 .114 .159 .223		061 .050 .457 .618 1.15 1.59 1.94 1.90 1.87 1.77 1.59	58.3 67.8 82.0 74.3 64.8 79.9 73.9 75.1

TABLE II.- EXPERIMENTAL RESULTS, CONE, FINENESS RATIO 4

М	α	CL	c_{D}	Cm	L/D	c.p.	М	α	$c_{ m L}$	c_{D}	Cm	L/D	c.p.
2.75	-1.0	-0.028	0.064		-0.433		4.48	-1.0	-0.030	0.060	4	-0.495	
	0	0	.063		0			-1.0	028	.063		449	
	1.0	.028		-0.017	.417	58.2		0	. 0	.059		0	
	3.0	.087	.075	058	1.16	64.2		1.0	.023	.062		•375	
	5.1	.150	.081	103	1.86	65.8		2.8	.072	.071	-0.050		66.9
	5.1	.161	.081	112	2.00	66.5		5.0	.195	.073	166	2.67	82.6
	7.6	.247	.097	173	2.55	66.9		7.8	.301	.109	245		78.3
	10.2	.349	.125	249	2.78	67.9		8.3	.281	.117	209		70.9
	10.4	.358	.131	259	2.73	68.9	-5	10.3	.366	.149	269	2.46	69.4
	12.7	.458	.168	329	2.72	68.0		11.8	.384	.173	275	2.22	66.9
	15.2	.596	.234	431	2.55	67.8		13.2	.460	.196	336		68.2
	15.3	.585	.230	426	2.55	68.1		15.3	.544	.254	404		68.3
	20.2	.848	.405	638	2.10	68.2	19	17.1	.619	.306	460		67.1
	25.3	1.067	.623	840	1.71	68.3		18.1	.668	.342	501	1.95	67.6
								20.1	.751	.412	572		67.5
4.01	-1.0	025	.054		460			22.1	.822	.488	641	1.68	67.8
	0	.015	.051		.290					-			
	1.0	.040	.056	033	.730		5.00	85	018	.064		285	
	3.0	.100	.065	102	1.54	76.3		.13	.010	.065		.149	
	3.0	.099	.063	072	1.57	70.4		1.1	.037	.062	028		74.3
	4.0	.128	.067	092	1.91	69.4		1.9	.057	.067	047		
640	5.0	.168	.074	122	2.26	70.4		2.4	.123	.059	100	2.08	79.9
	6.3	.219	.083	151	2.62	66.7		4.9	.208	.081	168		78.5
	7.0	.239	.090	170	2.65	68.7		6.8	.268	.104	205		73.7
	8.1	.277	.101	193	2.74	66.9		7.1	.221	.099	152		65.
	10.1	.360	.124	255	2.90	67.7		9.4	.298	.127	197	2.35	62.6
	10.4	.380	.144	277	2.64	69.2		9.4	.298	.114	198	2.62	63.3
	11.4	.394	.150	276	2.62	66.4		10.9	.349	.168	250		66.8
	12.2	.445	.166	320	2.68	68.0		13.3	• 473	.228	379		73.8
	13.9	.518	.208	379	2.49	68.5		15.3	.548	.292	438		72.3
	15.4	.560	.239	400	2.34	66.4		17.1	.613	.343	495		72.0
	16.1	.638	.292	471	2.18	67.9		17.9	.596	•353	422		62.1
	19.4	.721	.361	533	2.00	66.6		19.9	.677	.418	478		61.1
1 19	20.2	.787	.424	598	1.86	67.6		21.8	.738	.496	546	1.49	62.8
1 500	24.2	.939	•597	755	1.57	68.6						la de la constante de la const	

TABLE III.- EXPERIMENTAL RESULTS, CONE, FINENESS RATIO 5

M	α	c_{L}	$C_{\mathbb{D}}$	Cm	L/D	c.p.	M	α	CL	c_{D}	Cm	L/D	c.p.
2.75	-1.0 0 1.0 3.0	-0.032 002 .025 .092	0.058 .057 .057 .060		-0.548 035 .442 1.54		4.01	12.1 13.9 15.6 16.0	0.483 .561 .676 .680	0.155 .215 .279 .268	-0.346 410 513 494	2.61	68.6 68.8 70.8 67.9
	5.0 5.0 7.6 10.1	.161 .163 .249	.067 .064 .082	 -0.112 172 260	2.40 2.53 3.02 3.27	66.5 66.7 67.5	4.48	20.0 23.6	.858 1.022	.416 .579	639 790	2.06	67.3
	12.6 15.0 15.2 15.7 20.1 23.2	.499 .651 .670 .677 .941 1.123	.156 .221 .231 .245 .413	352 462 488 494 687 841	3.20 2.95 2.91 2.76 2.28 1.99	67.6 67.4 69.0 68.8 66.7 67.3	7.40	1.0 2.3 2.8 5.1 7.5 7.9	008 .022 .056 .079 .155 .252	.042 .045 .049 .052 .062 .080		183 .488 1.14 1.53 2.49 3.16	79.9 73.9 67.4 71.3
3.49	-1.0 0 1.0 3.0 5.0 5.0 7.6	030 .001 .027 .094 .160 .160	.053 .051 .052 .055 .062 .061	 018 067 109 109	558 .015 .529 1.71 2.59 2.63 3.22	63.6 69.4 66.6 66.6 67.7		10.0 12.6 13.1 15.2 17.2 17.4	•361 •486 •540 •636 •732 •734	.117 .172 .236 .250 .324 .321	251 342 391 490 564 542	3.08 2.82 2.29 2.55 2.26	66.7 66.8 67.4 72.1 71.0 68.1
	10.1 12.6 15.0 15.2 20.1 22.6	•372 •504 •628 •643 •874 1•037	.113 .167 .290 .236 .478 .553	266 361 460 468 658 810	3.28 3.02 2.16 2.72 1.83 1.88	68.8 68.3 67.4 68.6 66.8 69.2	5.00	85 .13 1.1 1.9 3.2 5.0 6.7	026 .003 .029 .052 .093 .155 .218	.050 .048 .054 .049 .054 .069	 068 119 171	2.24	71.1 74.4 75.8
4.01	-1.0 0 1.0 2.5 3.1 4.0 5.1 6.3	027 .002 .025 .074 .107 .126 .179 .219	.043 .050 .055 .052 .059 .062 .065	 059 - 078 - 093 - 130 - 153 - 182	-538 039 505 1.34 2.06 2.14 2.89 3.36 3.41	76.9 71.2 71.7 70.5 68.0 69.2		7.5 9.4 11.0 13.3 15.2 17.2 17.2 19.7 21.6	.233 .307 .380 .530 .608 .722 .727 .832 .899	.095 .124 .128 .190 .250 .329 .339 .434 .516	137 190 231 419 491 582 528 636 683	2.46 2.47 2.96 2.79 2.43 2.20 2.14 1.92	56.5 58.7 58.0 75.0 75.3 73.9 66.4 68.4 66.3
	8.1	•290 •375	.084	203 267	3.46 3.37	67.8 68.6		1.0					

TABLE IV.- EXPERIMENTAL RESULTS, CONE, FINENESS RATIO 7

M	α	C_{L}	c_{D}	C_{m}	L/D	c.p.	М	α	$c_{ m L}$	c_{D}	Cm	L/D	c.p.
2.75	-1.0 0 1.0 3.0 5.1 5.3 10.3 15.5 -1.0 0 1.0 3.0	-0.035 0 .030 .096 .162 .180 .434 .811 030 .004 .035 .101 .136	.046 .049 .047 .050 .062 .114 .248 .045 .046 .044	0.017 061 104 134 301 568	2.03 3.22 2.88 3.83 3.27 664 .095 .803 2.40	56.8 62.3 62.6 72.2 67.4 67.0	5.00	5.1 7.1 10.4 13.4 85 .13 1.1 2.4 4.9 6.8 8.0 9.9	.260 .462 .654	0.052 .066 .115 .184 .039 .037 .046 .049 .062 .074 .106		3.94 4.02 3.55 066 .620 1.13 1.90 2.79 3.27 2.53 3.10	

TABLE V.- EXPERIMENTAL RESULTS, 3/4-POWER BODY, FINENESS RATIO 3

М	α	$c_{ m L}$	c_{D}	C _m	L/D	c.p.	M	α	c_{L}	c_{D}	Cm	L/D	c.p.
2.75	-1.0 0 1.0 3.0 5.1 5.3 7.8 10.4 10.4 12.9 15.2 15.4 15.5 20.2 25.3	-0.027 .002 .030 .091 .154 .166 .247 .343 .354 .446 .551 .562 .549 .772 .948	0.080 .081 .089 .096 .095 .113 .144 .180 .237 .242 .244 .393 .588		-0.337 .028 .378 1.02 1.61 1.75 2.18 2.39 2.46 2.47 2.32 2.32 2.25 1.96 1.61		4.01 5.00	7.0 8.3 10.3 12.4 14.1 15.4 16.1 20.2 24.2 85 .13 1.1 1.9 2.5 4.9		0.102 .110 .141 .173 .206 .251 .270 .395 .536 .082 .080 .071 .075 .084	-0.147 175 226 278 324 366 400 502 623	2.45 2.44 2.38 2.30 2.14 2.09 1.79	64.6
4.01	-1.0 0 1.0 3.0 3.0 4.0 5.0 6.5	023 006 .031 .091 .092 .121 .158 .213	.071 .072 .072 .078 .074 .082 .072	 025 061 059 082 100 134	327 084 .426 1.16 1.24 1.47 2.22 2.32	76.5 64.7 61.8 64.8 60.9 60.3		6.6 7.4 9.7 11.2 17.5 20.0 22.0	.208 .232 .297 .334 .529 .623	.105 .123 .148 .179 .315 .396 .472	138 151 192 196 322 413 473	1.98 1.88 2.00 1.87 1.68 1.57	63.2 61.2 60.5 54.1 53.7 57.3 58.0



TABLE VI.- EXPERIMENTAL RESULTS, 3/4-POWER BODY, FINENESS RATIO 5

М	α	$c_{ m L}$	c_{D}	$C_{\mathbf{m}}$	L/D	c.p.	М	α	$c_{ m L}$	c_{D}	Cm	L/D	c.p.
2.73	-1.0 0 1.0 3.0 5.0 5.1 7.6 10.1 12.7 15.0	-0.035 002 .028 .097 .170 .167 .262 .390 .541 .714	0.043 .034 .044 .053 .061 .060 .079 .112 .162	0.055 110 098 167 253 356 468	3.31 3.48 3.33 3.04	 55.2 63.1 56.7 61.9 62.6 63.1 62.4	5.00	8.1 10.1 12.1 13.9 16.0 20.0 23.1 85	.415 .523 .611 .726 .921 1.083 006	.118 .157 .202 .272 .429 .578 .041 .036	495 638 775	3.52 3.33 3.02 2.67 2.15 1.87	63.7 64.7 64.8 64.3 64.0 63.2 63.5
4.01	15.2 20.1 -1.0	.718	.243 .448	484 730	1 /-			1.1 1.9 2.5 5.0 6.7	.042 .076 .090 .185	.058		1.09 1.96 1.95 3.19 3.11	
	0 1.0 3.0 3.1 4.0 5.1 6.3	.002 .028 .097 .105 .134	.034 .040 .046 .046 .050	019 060 068 080 118 156	.051 .712 2.11 2.30 2.71 3.21 3.63			7.0 9.4 10.7 15.2 17.2 17.2 19.6 21.6	.267 .360 .431 .681 .727 .769 .845	.131 .162 .311 .357 .375	247 298 497 502 563	2.74 2.66 2.19 2.04 2.05 1.87	

TABLE VII.- EXPERIMENTAL RESULTS, 1/2-POWER BODY, FINENESS RATIO 3

М	α	$c_{ m L}$	C_{D}	C_{m}	L/D	c.p.	М	α	CL	c_{D}	Cm	L/D	c.p.
4.01	-1.0 0 1.0 3.0 5.1 5.3 7.8 10.4 15.2 15.5 20.2 25.3 -1.0 0 1.0 3.0 5.0 6.5 7.0 8.3 10.3 12.4	-0.32 0 .031 .100 .168 .177 .272 .392 .599 .620 .839 1.031 -023 .005 .033 .094 .095 .126 .135 .220 .233 .280 .351 .425	.100 .109 .107 .133 .171 .262 .277 .430 .629 .086 .088 .091 .093 .098 .102 .100 .118 .129 .158	0.022 064 101 103	.333 .999 1.54 1.66 2.05 2.30 2.29 2.24 1.95 1.64 272 .062 .372 1.04 1.02 1.29 1.32 2.20 1.98 2.17 2.22	68.3 60.6 57.0 55.2 55.7 57.7 58.4 58.1 54.0 55.8 40.4 55.6 56.1 56.1 56.1 56.6 57.6	4.01	14.1 15.4 16.1 20.2 20.2 24.2 85 .13 1.1 1.9 2.5 4.9 6.6 7.8 9.7 11.2 13.3 15.3 17.3 17.5 20.0 22.0	0.491 .575 .586 .749 .760 .882 008 .010 .037 .055 .064 .148 .193 .231 .295 .349 .421 .515 .603 .536 .653 .737	0.229 .279 .291 .423 .432 .577 .099 .096 .098 .098 .117 .119 .142 .169 .192 .227 .289 .354 .342 .431	-0·308 364 369 490 489 614 	2.06 2.01 1.77 1.76 1.53 080 .100 .380 .579 .654 1.26 1.62 1.62 1.75 1.82 1.78 1.78 1.70	57.9 57.8 57.3 57.7 56.7 59.0



TABLE VIII.- EXPERIMENTAL RESULTS, 1/2-POWER BODY, FINENESS RATIO 5

М	α	c_{L}	$C_{\mathbb{D}}$	Cm	L/D	c.p.	М	α	$C_{\mathtt{L}}$	c_{D}	c_{m}	L/D	c.p.
2.75	-1.0 -0 0 1.0 3.0 5.1 5.1 7.6 10.1 12.4 15.0		0.051 .051 .052 .054 .066 .089 .130 .188 .279 .514 .045 .046 .046 .052 .057 .076 .077	-0.017 052 091 101 160 254 355 479 811	2.02 2.79 2.81 3.35 3.43 3.25 2.92 2.44 669 .132 2.24 2.51 3.75 4.42 3.39 3.33	48.2 46.0 47.7 51.0 52.0 54.7 55.8 55.7	5.00	13.9 16.0 20.1 23.1 85 .13 1.1 1.9 2.4 5.0 6.9 7.7 9.4 11.0 13.3 15.2 17.1 17.2 19.7 21.6	.805 1.038 1.213	.309 .488 .643 .060 .056 .058 .062 .052 .069 .090 .111 .145 .203 .245 .308 .302 .370 .373 .480	183 269 361 443 547 581 581	2.60 2.12 1.89 258 .115 .490 .758 1.24 2.25 2.69 2.71 2.52 2.26 2.28 2.21	

TABLE IX.- EXPERIMENTAL RESULTS, TANGENT OGIVE, FINENESS RATIO 3

M	α	CL	c_{D}	Cm	L/D	c.p.	М	α	$c_{ m L}$	c_{D}	C _m	L/D	c.p.
2.75	-1.0 0 1.0 3.0 5.0 5.3 7.8 10.4 10.4 13.0 15.2 15.5 15.5 20.2 25.3	-0.028 .004 .044 .114 .188 .196 .293 .396 .410 .502 .618 .615 .634 .848 1.040	0.113 .108 .113 .117 .131 .124 .153 .190 .198 .233 .293 .293 .299 .460 .668		1.84	54.8 54.3 54.0 56.3 56.4 54.4 56.8 57.1 57.2 56.2 58.0 58.0	5.00	10.3 12.4 14.1 15.4 16.1 19.5 20.2 24.2 85 .13 1.1 1.9 2.5 4.9	0.373 .450 .517 .578 .601 .735 .755 .884 004 016 .003 .058 .045 .123	0.175 .209 .246 .294 .311 .418 .443 .592 .114 .110 .113 .117 .106 .122	.032	2.16 2.10 1.97 1.94 1.76 1.71 1.49 038 148 .030 .493 .423 1.01	54.7 56.5 57.5 55.2 55.4 56.4 56.3 57.6
4.01	-1.0 0 1.0 3.0 3.0 4.0 5.0 6.5 7.0 8.3	027 .007 .031 .104 .116 .139 .217 .241 .289	.104 .103 .104 .111 .103 .115 .114 .123 .134		261 .064 .299 .936 1.13 1.20 1.89 1.96 2.16 2.05			6.6 7.9 9.7 11.2 13.3 15.3 17.3 17.5 20.0 22.0	.183 .289 .328 .385 .432 .503 .598 .503 .609 .688	.136 .149 .205 .225 .243 .301 .368 .358 .444 .513	096 189 232 306 355 422 248 338 400	1.94 1.60 1.71 1.78 1.68 1.62 1.40	48.8 61.6 52.8 55.0 64.2 62.9 62.0 42.1 46.7 48.2

48.8

56.5

55.8

60.5

60.5

60.6

NACA

-.216 2.32

-.363 2.22

-.432 2.16

-.515 2.10

-.623 1.89

-.727 1.76

.417

.597

.712

.778

.918

1.047

10.7

13.3

15.3

17.2

19.7

21.6

.180

.269

.329

.369

.595

L/D C_{m} c.p. L/D C_{T_1} CD M α C_{D} C_{m} c.p. CT. α 0.103 -0.190 3.45 51.8 4.01 8.1 0.355 0.806 -0.045 0.056 .141 -.266 3.30 55.0 10.1 .466 .053 -.023 0 -.001 -.335 3.17 55.5 .578 .182 12.1 .726 .054 1.0 .039 -.408 2.97 56.8 13.9 .684 .230 .066 1.84 3.0 .121 -.508 2.55 57.8 16.0 .822 .322 2.76 56.0 .077 0.123 5.1 .213 57.6 .495 -.657 2.09 1.034 57.4 20.1 3.35 .102 -.202 7.6 .342 -.838 1.72 58.2 24.6 .725 1.250 57.6 .146 -.286 3.29 .479 58.0 .158 3.22 -.307 .510 -.663 -.85 .053 5.00 -.035 .208 58.5 3.11 .648 -.397 .13 -.006 .052 -.126 .294 2.81 .826 .108 .006 .053 1.1 .294 2.85 59.1 -.523 .839 .601 .034 .057 1.9 .532 -.861 2.45 61.5 1.303 1.67 .062 3.0 .103 .699 2.20 61.0 -1.030

M 2.75 -1.0 10.2 10.5 12.7 15.1 15.3 20.2 23.6 1.539 .082 2.20 .181 4.9 - 2.20 6.6 .255 .116 - --.839 -.040 .047 4.01 -1.0 -.114 2.15 43.2 .117 6.9 .252 .048 0 -.118 2.18 .258 .118 43.6 7.2 .051 -.022 .712 1.0 .036 -.182 2.39 .147 49.1 9.4 .351 .761 -.019 50.7 1.0 .037

48.4

56.5

50.1

55.6

50.6

56.6

1.66

2.16

2.39

2.96

3.34

3.39

.058

.060

.067

.074

.083

.092

.096

.131

.159

.219

.277

.310

2.5

3.1

4.0

5.1

6.3

7.1

-.048

-.076

-.082

-.125

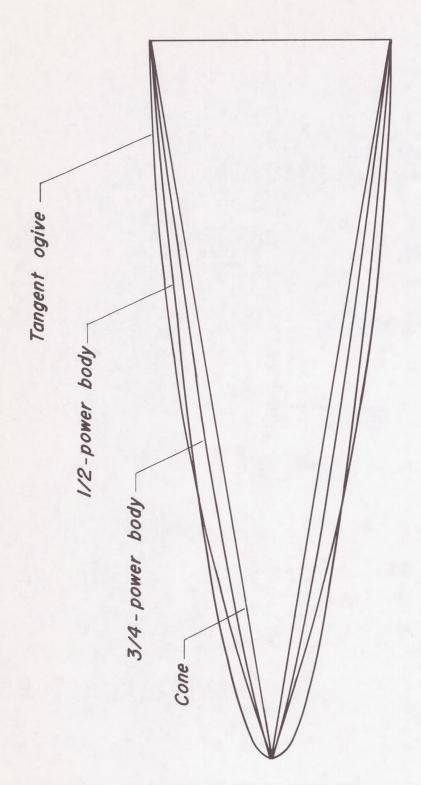
-.144

-.181

TABLE X.- EXPERIMENTAL RESULTS, TANGENT OGIVE, FINENESS RATIO 5

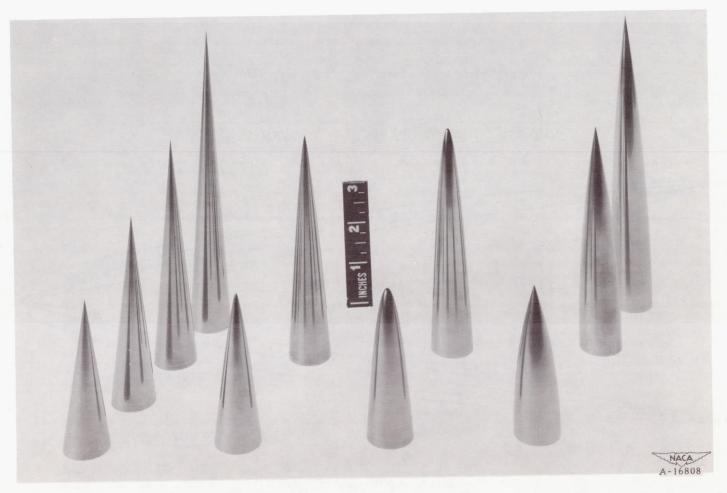
TABLE XI.- EXPERIMENTAL RESULTS, TANGENT OGIVE, FINENESS RATIO 7

М	α	$c_{ m L}$	c_{D}	$C_{\mathbf{m}}$	L/D	c.p.	М	α	$c_{ m L}$	$C_{\mathbb{D}}$	Cm	L/D	c.p.
2.75	0 1.0 3.0 5.1 5.3 10.5 13.0	-0.039 005 .036 .124 .214 .233 .563	0.045		2.40 3.45 3.26 3.84	41.6 49.1 50.2 54.3 57.0 57.5	4.01	5.1 6.3 7.2 10.4 13.5 85 .13 1.1 1.9 2.4 4.9 6.9 8.5	0.228 .305 .341 .574 .808	0.063 .076 .081 .152 .243 .041 .040	-0.130 183 173 349 499 021 033 044 125 212	3.65 3.98 4.21 3.79 3.32 463 .410 1.04 1.66 1.86 2.96 3.30	56.0 58.6 49.6 59.0 59.3
	1.0	.049 .135 .136	.047 .052 .051	027 070 077	1.04	54.0		6.9	.324	.098	212 236	3.30	+



(a) Profiles of fineness ratio 3 bodies.

Figure 1.- Test bodies of revolution.



Cones 3/4—power bodies 1/2—power bodies Tangent ogives

(b) Test bodies of revolution of fineness ratios 3, 4, 5, and 7.

Figure 1.— Concluded.

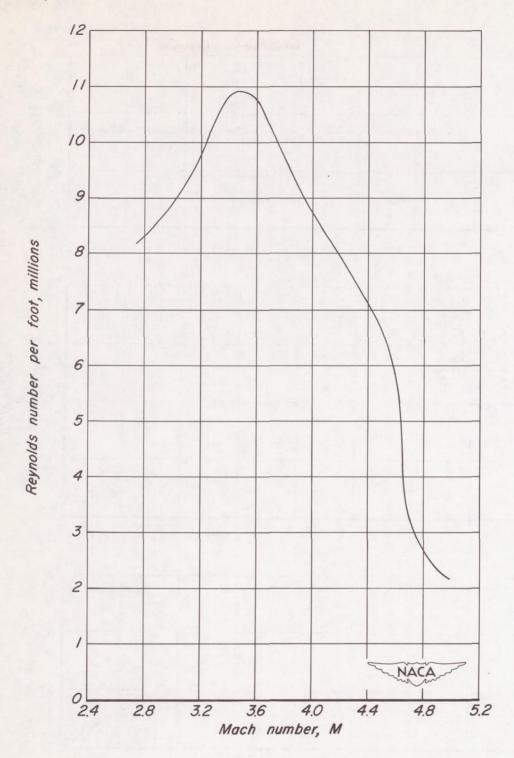


Figure 2.- Variation of Reynolds number with Mach number in the Ames 10- by 14- inch supersonic wind tunnel.

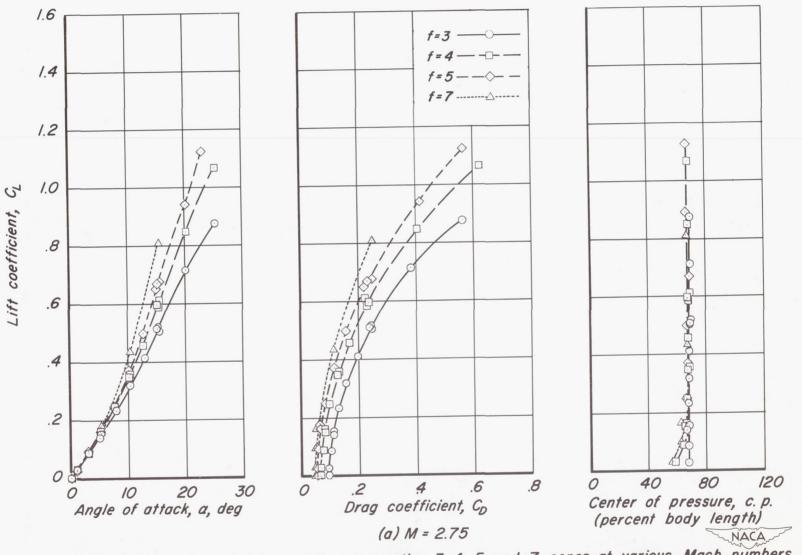


Figure 3.- Aerodynamic characteristics of fineness ratios 3, 4, 5, and 7 cones at various Mach numbers.

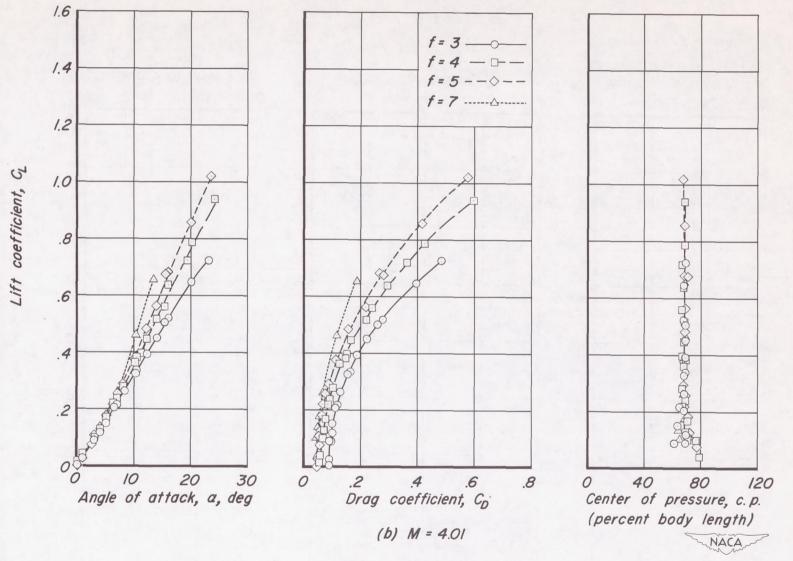
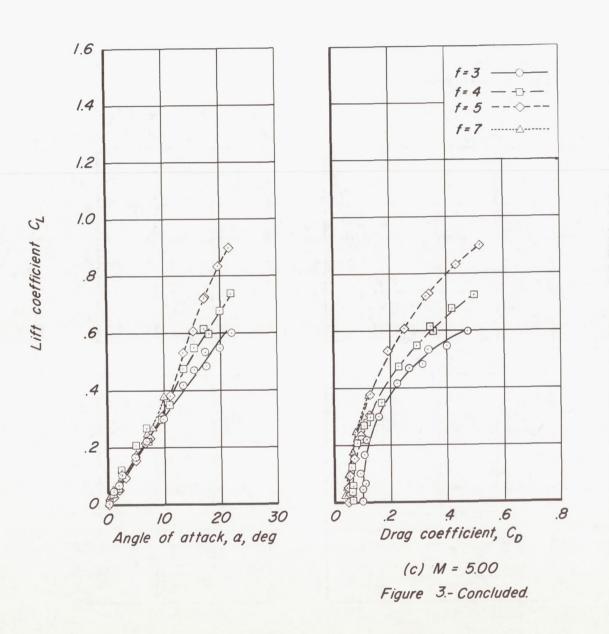


Figure 3.-Continued.



Center of pressure, c.p. (percent body length)

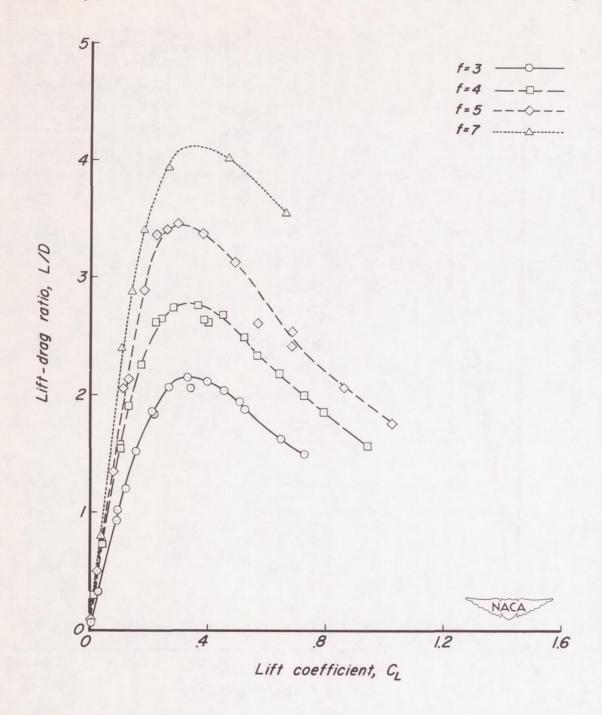


Figure 4.-Variation of lift-drag ratio with lift coefficient for fineness ratios 3, 4, 5, and 7 cones at Mach number 4.01.

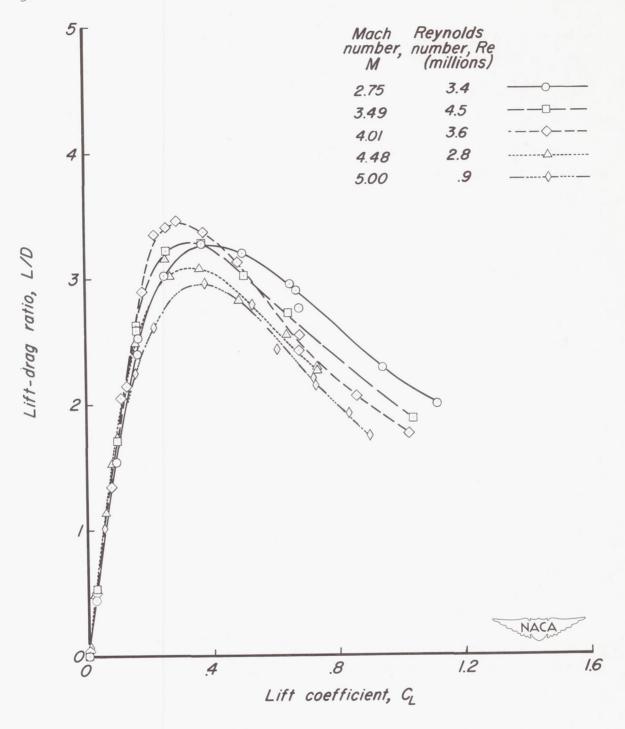


Figure 5.- Variation of lift-drag ratio with lift coefficient for the fineness ratio 5 cone at various Mach numbers.

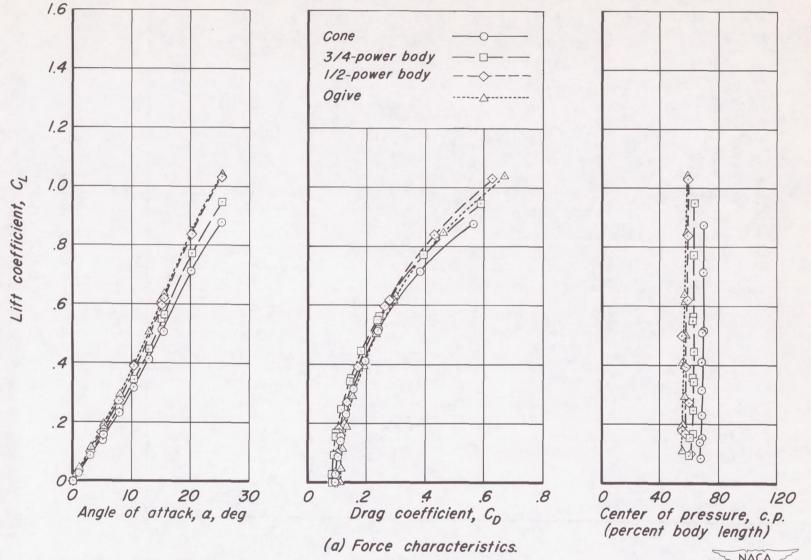
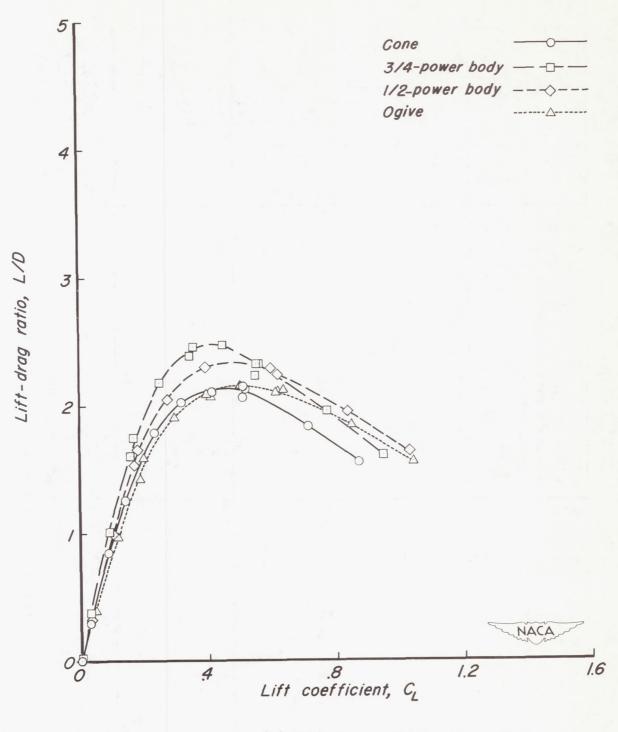


Figure 6.- Aerodynamic characteristics of fineness ratio 3 bodies at M = 2.75.



(b) Lift-drag ratios. Figure 6.- Concluded.

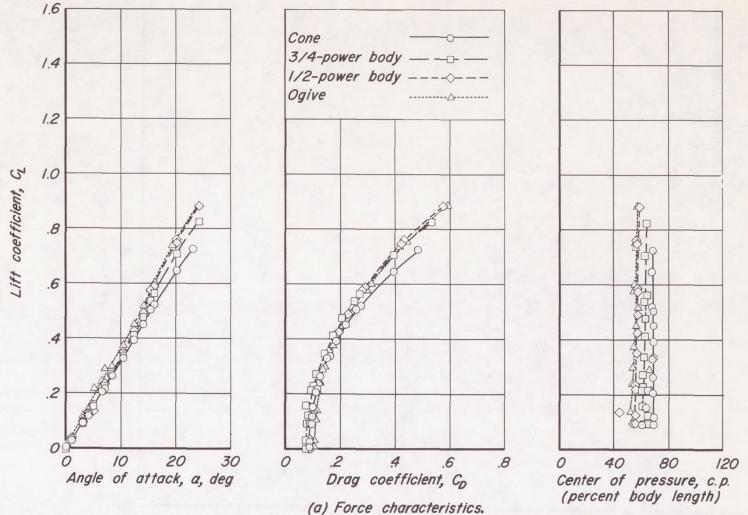


Figure 7.-Aerodynamic characteristics of fineness ratio 3 bodies at M = 4.01.

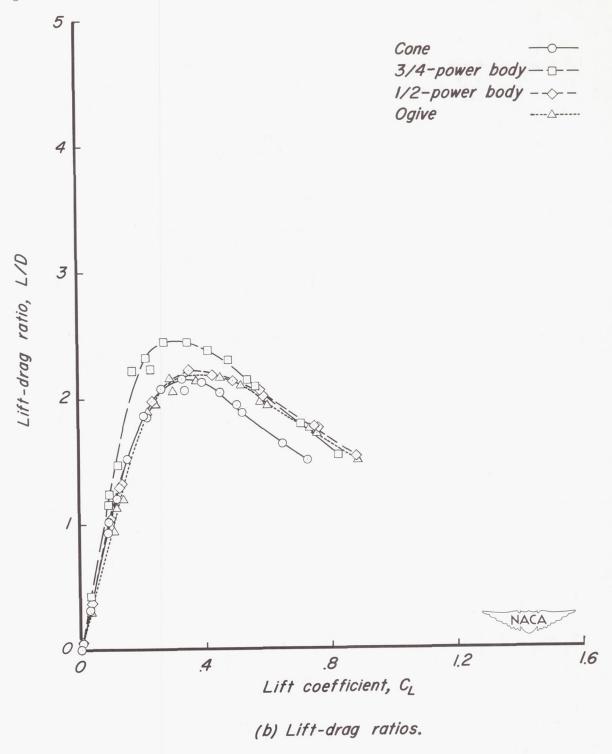


Figure 7.-Concluded.

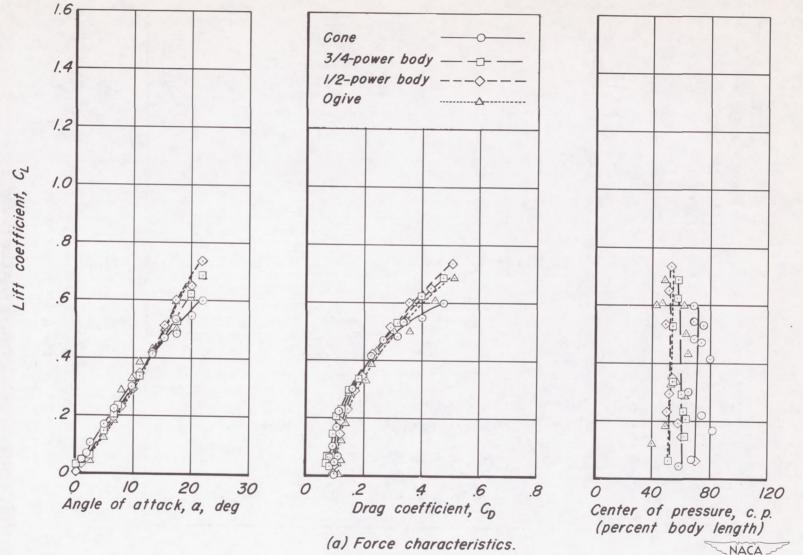
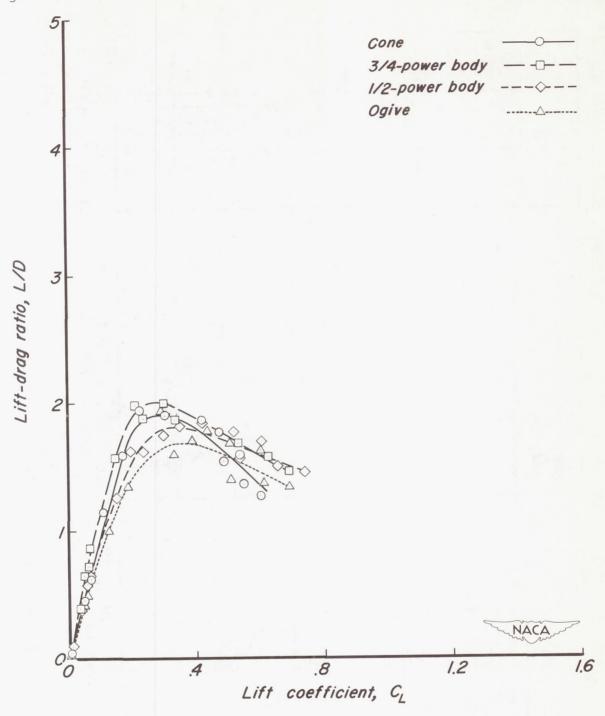


Figure 8.- Aerodynamic characteristics of fineness ratio 3 bodies at M = 5.00.



(b) Lift-drag ratios.

Figure 8.-Concluded.

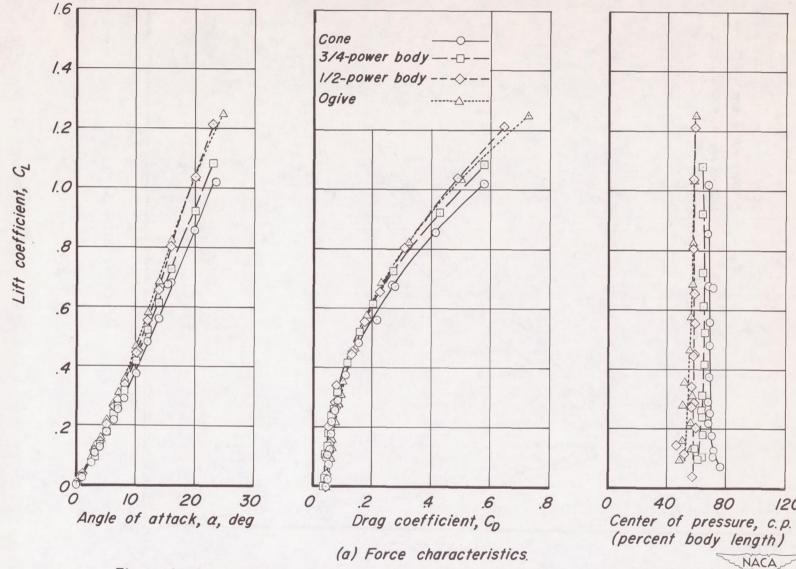


Figure 9.- Aerodynamic characteristics of fineness ratio 5 bodies at M = 4.01.

120

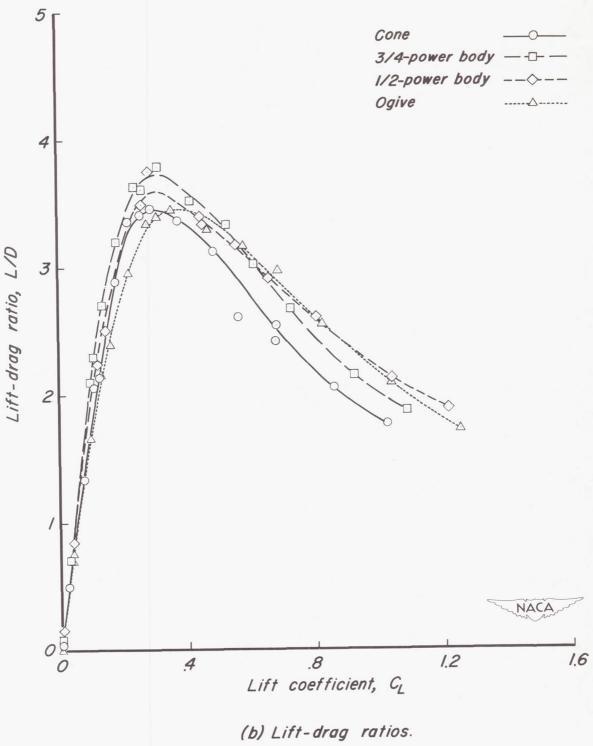


Figure 9.- Concluded.

0

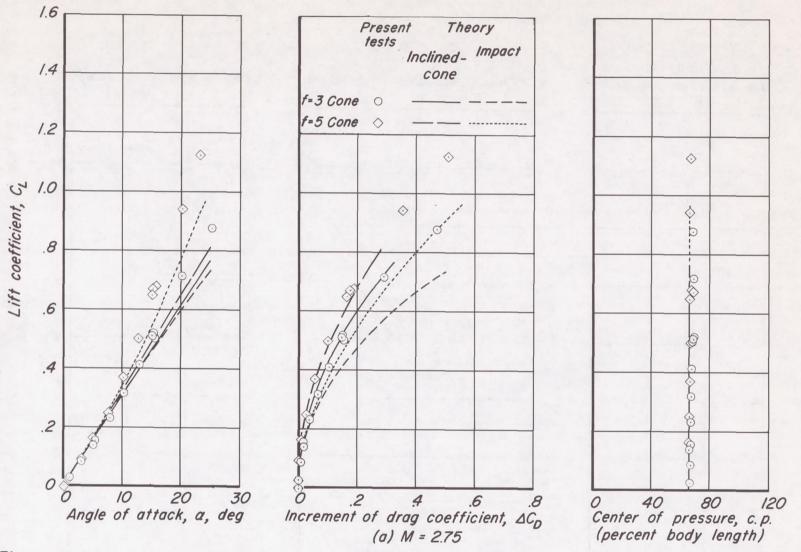
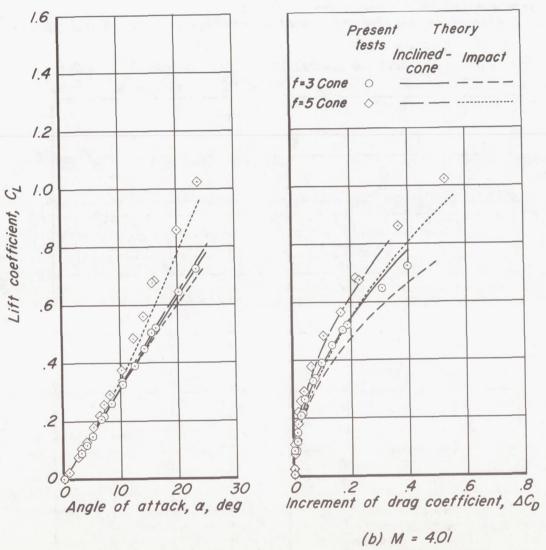
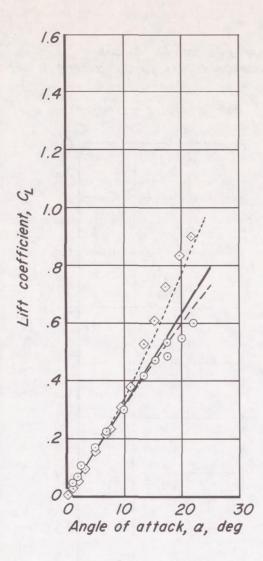


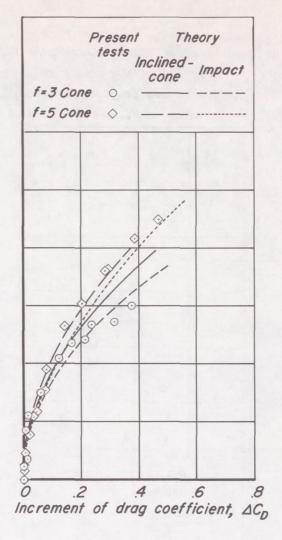
Figure 10.- Comparison of theoretical and experimental aerodynamic characteristics of fineness ratios 3 and 5 cones for various Mach numbers.



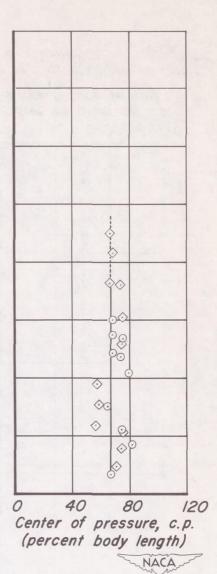
0 O 40 80 12 Center of pressure, c.p. 120 (percent body length)

(b) M = 4.01 Figure 10.- Continued.





(c) M = 5.00 Figure 10.-Concluded.



43

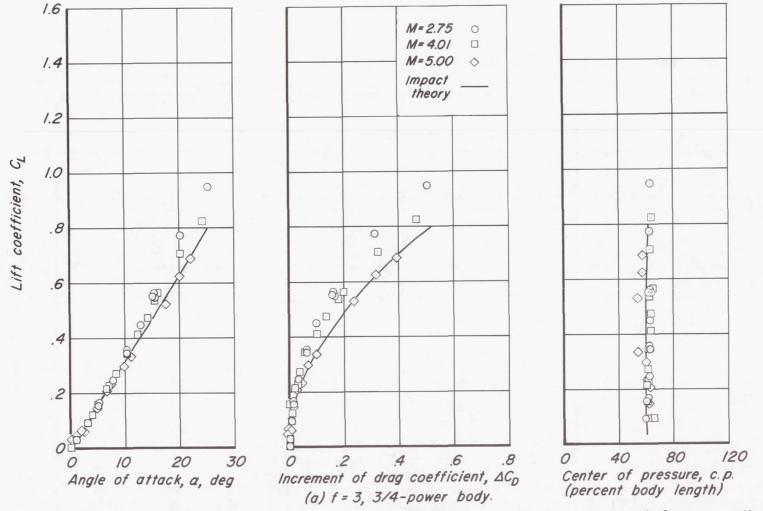
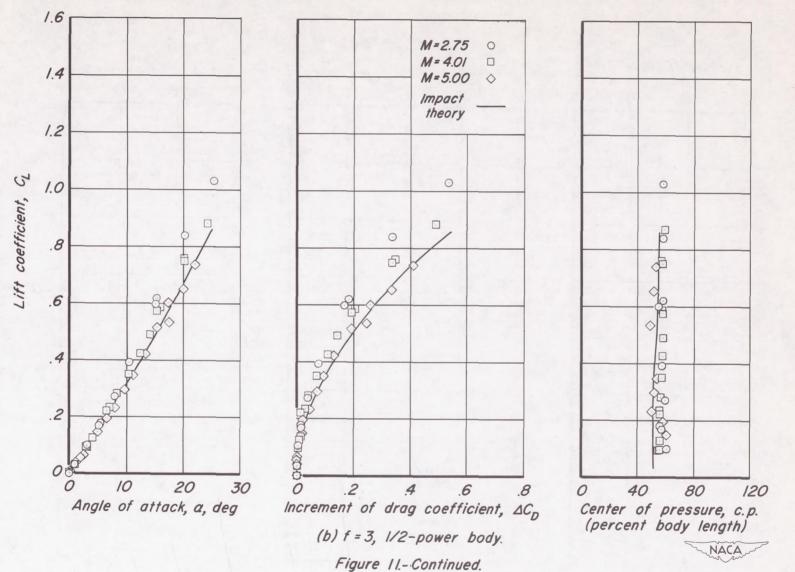
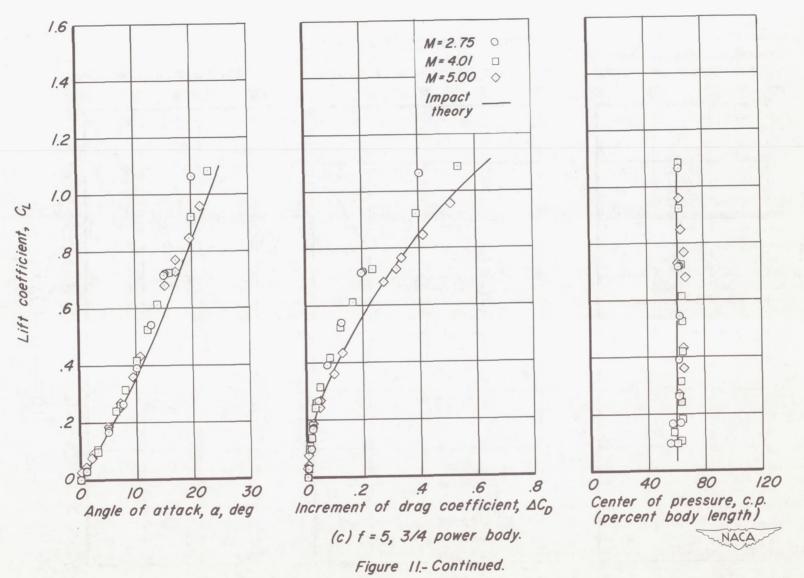
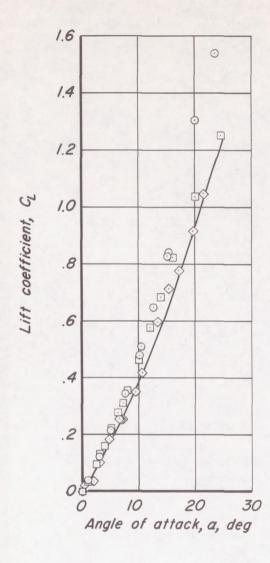
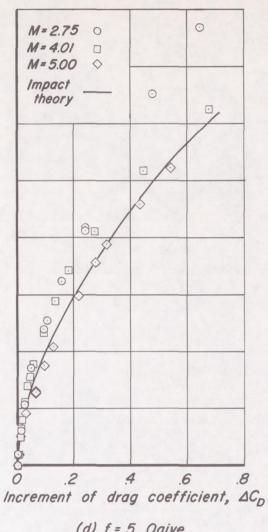


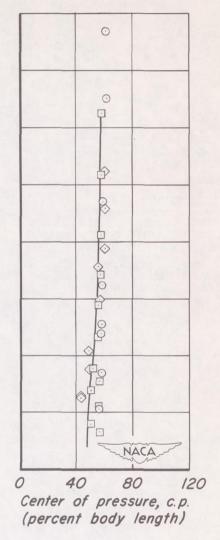
Figure II.-Comparison of typical theoretical and experimental aerodynamic characteristics of fineness ratios 3 and 5 ogives and blunt-nosed bodies at Mach numbers 2.75, 4.01, and 5.00. NACA











(d) f = 5, Ogive.
Figure 11.-Concluded.